EHD2 Interacts with the Insulin-Responsive Glucose Transporter (GLUT4) in Rat Adipocytes and May Participate in Insulin-Induced GLUT4 Recruitment †

ARTICLE *in* BIOCHEMISTRY · JULY 2004

Impact Factor: 3.02 · DOI: 10.1021/bi049970f · Source: PubMed

EHD2 Interacts with the Insulin-Responsive Glucose Transporter (GLUT4) in Rat Adipocytes and May Participate in Insulin-Induced GLUT4 Recruitment†

Seung Y. Park,‡ Byoung G. Ha,‡ Guem H. Choi,‡ Jiwon Ryu,§ Beomsu Kim,§ Chan Y. Jung,§ and Wan Lee*,‡

Department of Biochemistry, College of Medicine, Dongguk University, Kyungju 780-714, Korea, and Biophysics Laboratory, VA Medical Center, Department of Physiology and Biophysics, School of Medicine, State University of New York at Buffalo, Buffalo, New York 14215

Received January 4, 2004; Revised Manuscript Received March 9, 2004

ABSTRACT: Insulin-induced GLUT4 recruitment to the plasma membrane involves GLUT4 trafficking through multiple subcellular compartments regulated by multiple proteins, many of which are yet to be identified. Here we describe a 65 kDa protein found in purified GLUT4 vesicles of rat adipocytes as a potential GLUT4 traffic regulatory protein. On the basis of MALDI-TOF MS, RT-PCR, gene cloning, protein sequencing, and immunoreactivity data, we identified this protein as EHD2, a member of the EH domain-containing proteins that have been implicated in vesicle trafficking. EHD2 in rat adipocytes was 85% membrane-associated, including approximately 10% in immunopurified GLUT4 vesicles. This association of EHD2 with GLUT4 vesicles occurred in PM and three distinct endosomal fractions and was not significantly affected by cellular insulin treatment. In co-immunoprecipitation experiments, however, EHD2 physically interacted with GLUT4 in each of these fractions, and cellular insulin treatment selectively enhanced this interaction in an endosomal fraction thought to contain GLUT4 exocytic vesicles. EHD2 also interacted with the clathrin adaptor middle chain subunit μ_1, μ_2, and rCALM in GST pull-down experiments. Significantly, an affinity-purified EHD2 antibody and a peptide corresponding to the EHD2 sequence Glu^{428}−Glu^{535} drastically (by 75% and 35%, respectively) suppressed the insulin-induced increase in the plasma membrane GLUT4 contents in SLO-permeabilized rat adipocytes without affecting the basal GLUT4 distribution. These findings strongly suggest that EHD2 interacts with GLUT4 in rat adipocytes and may play a key role in insulin-induced GLUT4 recruitment to the plasma membrane.

The stimulation of glucose uptake in adipose and muscle cells by insulin plays a key role in the whole-body glucose homeostasis (*1*). GLUT4, the major glucose transporter isoform expressed in these cells (*2*), is mostly stored in intracellular sites in the basal state, and insulin stimulates the glucose uptake in these cells primarily by recruiting GLUT4 from these storage sites to the plasma membrane (*3*). GLUT4 in these cells is also known to constantly recycle between the plasma membrane and the intracellular storage sites via endocytosis, exocytosis, and vesicle trafficking (*4*−*6*). In immunoelectron microscopy, GLUT4 in adipocytes is associated with a number of morphologically distinct membrane structures or compartments, including tubulovesicular elements, small vesicles, clathrin-coated vesicles, and plasma membrane invaginations (*7*, *8*), clearly suggesting that the GLUT4 recycling involves multiple endosomal compartments in addition to the plasma membrane.

Separation of individual endosomal GLUT4 compartments has been elusive. Subcellular membrane fractionation after cell homogenization has been successful in separating the plasma membrane (PM) from endosomal membranes (HDM and LDM) but less successful in separating individual compartments within the endosomal system because of vesiculation of endosomes caused by mechanical homogenization. Using hypotonic lysis rather than mechanical homogenization, we (*9*, *10*) have recently separated the intracellular GLUT4 store in rat adipocytes into three distinct fractions, T, H, and L, where H and L were released into medium as heavy and light fractions, respectively, while T was trapped inside the plasma membrane (PM) sheets of lysed cell residue (900*g* pellets or fraction G), and have shown that GLUT4 pool sizes in these fractions were characteristically affected by cellular insulin stimulation (*9*, *10*). These findings together with organelle-specific marker distribution data suggest that the GLUT4 pools in T, H, and L represent, respectively, sorting endosomes, GLUT4 storage endosomes, and GLUT4 exocytic vesicles. Further evidence suggests that GLUT4 cycles through PM, T, H, and L, in a simple, one-way linear fashion that is describable by four first-order rate coefficients, each of which is modulated during insulin-induced GLUT4 recruitment (*10*, *11*). The molecular mechanisms by which these GLUT4 transits are modulated during insulin-induced GLUT4 recruitment to the plasma membrane, however, are yet to be elucidated.

Studies with GLUT4-containing vesicles (IRGTV)[1] isolated after cell homogenization, on the other hand, have disclosed numerous proteins that reside in GLUT4 compartments (*11*−*33*). These include the vesicle fusion machinery

† This study was supported by a grant from the Korea Health 21 R&D Project, Ministry of Health and Welfare, Republic of Korea (00-PJ-3-PG6-GN07-0001), the American Diabetes Association, and Buffalo VA Medical Center Medical Research Services.

* Corresponding author. Tel: (054) 770-2409. Fax: (054) 770-2447. E-mail: wanlee@dongguk.ac.kr.

‡ Dongguk University.

§ State University of New York at Buffalo.

10.1021/bi049970f CCC: $27.50
Published on Web 05/15/2004

proteins such as VAMPs (*11*−*13*), secretory carrier membrane proteins, SCAMPs (*14*, *15*) and cellugyrin (*16*, *17*), endosomal markers such as the IGFII/Man 6-P receptor (*18*), transferrin receptor (*19*), and a neurotensin receptor, sortilin (*20*). While these proteins are known to be present in vesicles other than GLUT4 vesicles, insulin-responsive aminopeptidase (IRAP) colocalizes exclusively with GLUT4 and moves to the plasma membrane in response to insulin (*13*, *17*, *21*). A number of extrinsic membrane proteins are also known to associate with GLUT4-containing vesicles. These include acyl-CoA synthetase 1 (*22*), Akt-2/PKB (*23*, *24*), Rab4 (*25*), Rab11 (*26*), PI3 kinase (*27*), PI4 kinase (*28*), GDI (*29*), tankyrase (*30*), p62/CE (*31*), vimentin (*32*), α-tubulin (*32*), and the recently found unconventional myosin Myo1c (*33*). These lists are by no means exhaustive, and there are many more GLUT4 vesicle-associated proteins of unknown identity that may play a key role in modulating GLUT4 recycling and the insulin-induced GLUT4 recruitment.

In the present study, we describe a 65 kDa protein as a new member of the GLUT4 compartment-associated proteins in rat adipocytes. We identified this protein as EHD2, a member of a highly conserved family of Eps15 homology domain-containing proteins implicated in protein recycling. We also present a set of data to suggest that EHD2 may function as an adaptor protein involved in GLUT4 sorting into the clathrin-coated carrier vesicle formation required for the endosomal GLUT4 trafficking and recycling and may play a role in insulin-induced GLUT4 recruitment in rat adipocytes.

EXPERIMENTAL PROCEDURES

Materials. Collagenase type I was obtained from Worthington (Lakewood, NJ). The anti-GLUT4 monoclonal antibody (clone 1F8) (*34*) and anti-GLUT1 antibody were purchased from Biogenesis Ltd. (Sandown, NH). Antibody against rat adipose EHD2 was raised in rabbits using purified His fusion recombinant protein of rat adipose EHD2. A good titer level was obtained after two subsequent boosters with the protein in Freund's incomplete adjuvant. The IgG from antiserum was purified by protein A affinity chromatography according to the manufacturer's protocol (Amersham, NJ), and the antibody specificity was confirmed by immunoblotting. The polyclonal antibody against GLUT4 was the affinity-purified rabbit antibody raised using the carboxyl-terminal 11 amino acids of GLUT4. IRAP antibody was kindly given by Dr. Kozma (Metabolex Inc., Hayward, CA). Anti-rCALM antibody from rabbit was raised using a partial fragment (amino acids L^{396}−S^{531}) of rat brain rCALM (GI 2792500) GST fusion protein. Horseradish peroxidase-labeled protein A and anti-mouse IgG were from Zymed Laboratories Inc. (San Francisco, CA). Insulin (porcine crystalline) was purchased from Sigma (St. Louis, MO). Oligonucleotide primers were from Bionics (Seoul, Korea). All other chemicals were standard commercial products of reagent grade quality except for individually stated reagents listed below.

Subcellular Fractionation of Adipocytes. Adipocytes were isolated from epididymal fat pads of male Sprague-Dawley rats and stabilized as described (*35*). Subcellular membrane fractions enriched with plasma membranes (PM), nucleus/mitochondria (NM), high-density microsome (HDM), and low-density microsomes (LDM) were prepared after homogenation as described (*36*). Subcellular fractions from hypotonically lysed adipocytes were prepared as previously described using hypotonic lysing medium (0.25 mM ATP, 2.5 mM $MgCl_2$, 0.1 mM $CaCl_2$, 0.1 mM NAD, 0.05 mM NADP, and 1 mM $KHCO_3$, pH 7.4) (*9*). Briefly, adipocyte hypotonic lysates were centrifuged at 900*g* for 15 min, and the resulting pellet (900*g* pellet, denoted as G) was resuspended in 600 μL of NaCl/HEPES buffer (150 mM NaCl, 10 mM HEPES, 1 mM EGTA, and 0.1 mM $MgCl_2$, pH 7.4). The 900*g* supernatant was centrifuged at 185000*g* for 2 h, and the pellet (185000*g* pellet) was resuspended in 600 μL of NaCl/HEPES buffer. A suspension of 900*g* pellet (G) or 185000*g* pellet, without or after sonication, was then layered onto 9 mL of 5−30% glycerol gradient prepared in NaCl/HEPES buffer over 400 μL of 50% (w/v) sucrose pad in 10 cm height and centrifuged in a 40.2SW rotor (Beckman) at 60000*g* for 1 h, and 13 fractions were collected from the bottom to the top (P and 1−12). This typically separated GLUT4 into two peaks, a sharp, heavy peak (fractions P, 1, and 2), and a broad, light peak (fractions 3−12). They were separately pooled and designated respectively as fractions G_H and G_L for the 900*g* pellet (after sonication) and fractions H and L for the 185000*g* pellet.

Immunoadsorption. Immunoadsorptions were performed as described previously (*31*) with modifications. 1F8 or normal mouse IgG was coupled to Trisacryl beads (Reacti-Gel GF2000, Pierce) at a concentration of 1.0 mg of antibody/mL of resin according to the manufacturer's instructions. The antibody-coupled beads were quenched by 2 M Tris-HCl (pH 8.0) for 1 h, incubated with 2% BSA in PBS (134 mM NaCl, 2.6 mM KCl, 6.4 mM Na_2HPO_4, and 1.46 mM KH_2PO_4, pH 7.4) for 2 h to prevent nonspecific binding, and washed five times with 1 mL of PBS at room temperature. Three hundred micrograms of the homogenized membrane fraction (LDM) was incubated with 90 μL of beads overnight at 4 °C, and unbound supernatants were collected for analysis. For fractions G_L and L and sonicated fraction H, 200 μg of protein and 30 μL of beads were used for immunoadsorption. Beads were washed five times with 1 mL of PBS at 4 °C, and then the adsorbed material was eluted with SDS-containing (2%) Laemmli buffer without β-mercaptoethanol for 1 h at room temperature.

Gel Electrophoresis and Immunoblotting. Solubilized membrane in Laemmli solution was subjected to SDS−PAGE on 8% or 10% resolving gels as described (*37*). Separated proteins were electrophoretically transferred to nitrocellulose membrane (Bio-Rad, Hercules, CA), blocked with 5% nonfat milk in Tris-buffered saline, and incubated with primary antibodies in TTBS (Tris-buffered saline containing 0.05% Tween 20) containing 1% nonfat milk. After overnight incubation, membranes were washed with TTBS and incubated with horseradish peroxidase-labeled protein A (for the detection of polyclonal antibodies) or horseradish peroxidase-labeled anti-mouse IgG (for the

[1] Abbreviations: IRGTV, insulin-responsive glucose transporter vesicles; IRAP, insulin-responsive aminopeptidase; rCALM, rat clathrin-assembly lymphoid myeloid leukemia protein; GST, glutathione *S*-transferase; SLO, streptolysin O; MALDI-TOF MS, matrix-assisted laser desorption ionization time-of-flight mass spectroscopy; μ_1, the clathrin adaptor complex middle chain subunit 1; μ_2, the clathrin adaptor complex middle chain subunit 2.

detection of monoclonal antibodies). Proteins were visualized using an enhanced chemiluminescent substrate kit (NEN Life Science Products). Immunoblot intensities were quantitated by densitometry using an analytical scanning system (Molecular Dynamics Inc., Sunnyvale, CA).

MALDI-TOF MS Analysis. Proteins resolved by gel electrophoresis were visualized by silver staining (*38*) and rinsed with 1% acetic acid. Selected bands, including the one corresponding to 65 kDa, were excised into an Eppendorf tube with a clean scalpel, and 10 μL of 1% acetic acid was added. Protein samples were subjected to protein identification based on MALDI-TOF MS (Brucker Reflex III, Bremen, Germany) analysis after tryptic digestion (*39*).

RT-PCR and Cloning of Rat Adipose EHD2. Rat adipose tissues were homogenized with a tissue tearor in solution D containing 4 M guanidinium thiocyanate, 25 mM sodium citrate, 0.5% sarcosyl, and 0.1% β-mercaptoethanol (pH 7.0). Total RNA was extracted according to standard protocols (*40*). The quantity and quality of the isolated RNA were determined by absorbance at 260 and 280 nm. Poly(A)$^+$ RNA of rat adipose tissue was prepared using the FastTract 2.0 kit (Invitrogen, San Diego, CA) according to the manufacturer's recommendation. Avian myeloblastosis virus reverse transcriptase (2.5 units), *Tfl* DNA polymerase (Promega, Madison, WI), primers and 1.5 μg of poly(A)$^+$ RNA of rat adipose tissue were used for reverse transcription and amplification with a DNA thermal cycler (Perkin-Elmer Cetus, Warrington, U.K.). BLAST searches revealed that three peptides out of the four sequenced were homologous to sequences in human and mouse EHD2. On the basis of the conserved regions derived from arrangement between human and mouse EHD2 sequences, three primer sets were designed: 5′ EHD2-S1, ATGTTCAGTTGGCTGGGTAACG (397−418), and 3′ EHD2-S1, CGCATCAGCTGCTGGGTCTC (1069−1088); 5′ EHD2-S2, TCTACATTGGCTCCTTCTGGTCCC (1151−1174), and 3′ EHD2-S2, ACCACCCACTCGGCATCATCG (1699−1718); 5′ EHD2-S3, GATGATGCCGAGTGGGTGG (1699−1717), and 3′ EHD2-S3, GCTCTCTCATTCTGATACTTTCC (1988−2010) (see Figure 4 for nucleotide numbers). Rat adipocyte cDNA was amplified by PCR with three primer sets (2 min at 94 °C, then 30 cycles of 30 s at 94 °C, 30 s at 62 °C, and 1 min at 72 °C, followed by 10 min extension at 72 °C). The products were purified with a QIAquick gel extraction kit (QIAGEN, Alameda, CA) and sequenced. The sequence information was used to design primers for 5′ RACE PCR: 5′R-1, GAATCAGTGGTTGGCTCAGGC (663−683); 5′R-2, AGGTGGTCTTGCCAGTAGAGTATTG (592−616); 5′R-3, TGGTCTTGTAGAGTTTCTTGAGCCC (466−490). 5′ RACE was performed according to the manufacturer's instructions (Invitrogen, Carlsbad, CA). The 5′ RACE product gave the sequence from 1 to 490. The complete open reading frame of rat adipose EHD2 flanked with *Bam*H I and *Eco*R I restriction sites was generated by RT-PCR and inserted into the pGEX4T-1 vector. From the resulting clones the plasmids were purified and sequenced in both directions. A segment of EHD2 containing the Eps15 homology domain (Glu^{428}−Glu^{535}) was cloned into the pGEX4T-1 vector to obtain GST fusion protein (GST-ΔEHD2).

Fusion Protein Preparation and Purification. pGEX4T-1 plasmid containing the EHD2 or ΔEHD2 cDNA was transformed into the competent *Escherichia coli* BL21. Seed cultures in 100 mL of LB medium containing ampicillin (50 μg/mL) were obtained by inoculating one loop of *E. coli* BL21 containing pGEX4T-1/EHD2 or ΔEHD2 and incubating at 37 °C for 15 h. One liter of LB medium containing ampicillin (50 μg/mL) was inoculated with the seed cultures and cultured at 37 °C for 2.5 h. At that time, isopropyl 1-thio-D-galactopyranoside (IPTG, final concentration to 0.2 mM) was added, and the mixture was incubated for another 4 h. The cells were collected by centrifugation, washed with phosphate-buffered saline buffer (pH 7.3) on a GS-3 rotor for 10 min at 7700*g* at 4 °C, and stored at −70 °C until use. For the preparation of His fusion protein, the EHD2 cDNA was directionally subcloned in the *Bam*HI and *Eco*RI sites of the pET28a vector and transformed into the competent *E. coli* BL21. His fusion protein was induced by the addition of IPTG to 1 mM final concentration and purified by Ni−agarose beads (QIAGEN, Valencia, CA). The degree of purification was determined by using 10% SDS−PAGE and Western blot.

In Vitro Pull-Down Assay. Adipocytes were chilled and homogenized with STE buffer (250 mM sucrose, 20 mM Tris-HCl, 5 mM EGTA, and 2 mM EDTA, pH 7.5) containing 20 μg/mL aprotinin, 20 μg/mL leupeptin, 1 mM phenylmethanesulfonyl fluoride, and 1% Triton X-100. Homogenates were centrifuged first at 500*g* for 10 min to remove the fat cake and insoluble substances, and then the dissolved materials were centrifuged at 185000*g* for 2 h to obtain the supernatant (total cell lysates). Five micrograms of GST-μ_1, GST-μ_2, or GST-rCALM immobilized on glutathione−agarose beads was incubated with 1 mg of total cell lysates in 1 mL of 150 mM PBS at 4 °C for 3 h with end-over-end rotation. The beads were collected by centrifugation and washed three times with 1 mL of PBS. Proteins on the beads were eluted with 50 μL of 10 mM reduced glutathione in 50 mM Tris-HCl (pH 8.0) and subjected to protein analysis and Western blotting.

Streptolysin O (SLO) Permeabilization and Antibody Treatment. Adipocytes were permeabilized with SLO as described (*41*) with slight modifications. Adipocytes were washed with cold intracellular buffer (140 mM potassium glutamate, 20 mM HEPES, 5 mM $MgCl_2$, 5 mM EGTA, and 5 mM NaCl, pH 7.2) and incubated with intracellular buffer containing 200 units/mL SLO at room temperature for 15 min. Adipocytes were washed twice with intracellular buffer containing 1 mg/mL bovine serum albumin and the ATP-regenerating system (40 IU/mL creatine phosphokinase, 5 mM creatine phosphate, and 1 mM ATP) and incubated with 0.5 mg/mL anti-EHD2 antibody or normal rabbit IgG for 1 h at 37 °C. Where the dominant negative effect of ΔEHD2 was studied, 50 μM purified GST-ΔEHD2 or GST was incubated with adipocytes for 1 h at 37 °C. When specified, adipocytes were treated with insulin (100 nM) for the last 20 min of the semipermeabilization protocol above.

Statistical Analysis. Values are expressed as the mean ± SD. Where applicable, the significance of difference was analyzed using Student's *t* test for unpaired data.

RESULTS

Identification of a 65 kDa Protein in GLUT4 Vesicles as EHD2 in Rat Adipocytes. The GLUT4-containing vesicles immunopurified from rat adipocyte homogenates, widely

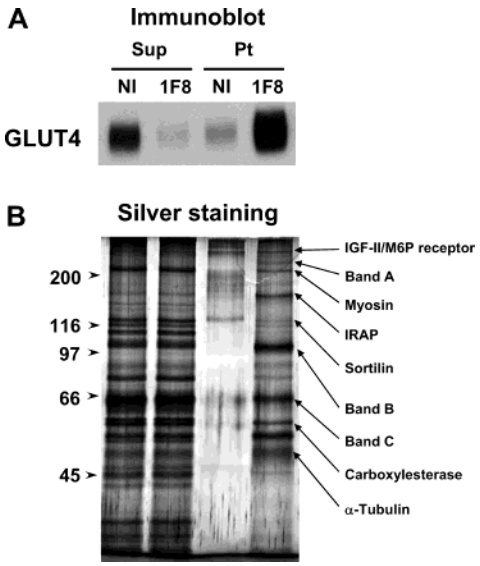

FIGURE 1: Protein composition and GLUT4 content of IRGTV immunopurified from rat adipocytes. Low-density microsomes were prepared from adipocytes, and each (500 μg of protein) was subjected to immunoadsorption with 1F8 (1F8) or normal mouse IgG (NI) (see Experimental Procedures). Immunoadsorbed materials (Pt) were eluted with SDS-containing Laemmli buffer without β-mercaptoethanol for 1 h at room temperature. After addition of β-mercaptoethanol (1% final) to the eluates, the proteins were resolved in SDS−PAGE in 8% gel and subjected to GLUT4 immunoblotting (panel A) and silver staining for protein analysis (panel B). Unadsorbed supernatants (Sup) were also subjected to protein staining and immunoblotting. One-fifth of adsorbed materials and $^1/_{50}$th of unadsorbed supernatants were used for analysis. The result shown here was representative of eight independent experiments. Those protein bands that were subjected to MALDI-TOF MS analysis are marked by arrows, with their identities when already available in the literature or with A, B, and C for the unidentified 230, 110, and 65 kDa proteins (panel B, right).

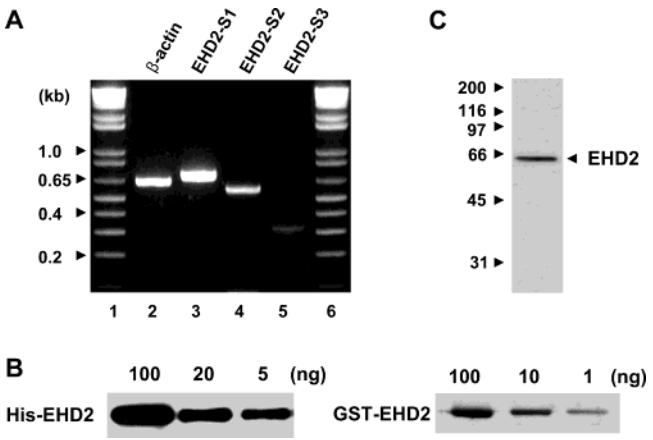

FIGURE 2: Identification of EHD2 in rat adipose tissue by RT-PCR and Western blot analysis. Panel A: RT-PCR analysis in poly-$(A)^+$ RNA from rat adipose tissue was done using the primers derived from sequences located in different conserved sites of EHD2 as described (see Experimental Procedures). 25 μL of PCR reactions was analyzed in a 1.5% agarose gel. EHD2-S1, EHD2-S2, and EHD2-S3 were amplified by EHD2-S1 5′ and 3′ primers (lane 3), EHD2-S2 5′ and 3′ primers (lane 4), and EHD2-S3 5′ and 3′ primers (lane 5), respectively. Lanes 1 and 6 were DNA size markers, while lane 2 contained control β-actin fragment as a control. Panel B: Using rat adipose EHD2 constructs cloned in pET28a (for His-EHD2) or pGEX4T-1 (for GST-EHD2) vectors, recombinant proteins were prepared, and anti-His-EHD2 antibody was produced as described in Experimental Procedures. The affinity of antibody was evaluated by Western blotting His-EHD2 and GST-EHD2 recombinant protein. Panel C: Total adipocyte lysates were prepared using a dissolving buffer containing 1% Triton X-100 as described in Experimental Procedures. 30 μg of the total cell lysate was subjected to 8% SDS−PAGE separation and then Western blotting using anti-EHD2 antibody as described in Experimental Procedures. Molecular marker positions are indicated by arrowheads.

known as IRGTV, contain many protein species of unknown identity, some of which are likely to play a critical role in GLUT4 traffic regulation and insulin-induced GLUT4 recruitment in this classical insulin target cell. In an effort to identify these putative, GLUT4 regulatory proteins, we have immunopurified GLUT4-containing vesicles (IRGTV) from LDM of rat adipocyte homogenates using GLUT4-specific antibody 1F8 immobilized on beads as described in Experimental Procedures. 1F8 beads adsorbed LDM GLUT4 vesicles almost quantitatively (more than 95%) under the conditions used (Figure 1A). More than a dozen protein bands were resolved on SDS−PAGE of purified IRGTV that were not present in control vesicles adsorbed to nonimmune IgG beads (Figure 1B), indicating that these proteins are specifically associated with GLUT4-containing vesicles.

Selected protein bands resolved on the SDS−PAGE of IRGTV as specified in Figure 1B were excised and digested with trypsin, and the peptide fragments were analyzed by MALDI-TOF MS for protein identification. Of nine discrete protein bands studied, six have been identified by various authors, namely, IGF-II/mannose 6-phosphate receptor (*18*), nonmuscle myosin (*33*), IRAP (*13*, *17*, *21*), sortilin (*20*), carboxyl esterase (*31*), and α-tubulin (*32*). The remaining three protein bands were identified as new members of the IRGTV-associated proteins. They migrated as apparent molecular masses of 230, 110, and 65 kDa on the SDS gel and are designated as bands A, B, and C, respectively, in Figure 1B. For the 65 kDa protein band (band C in Figure 1B), the linear tryptic spectra of nine potent peptide fragments were matched with the mouse EH domain-containing protein 2 (EHD2; GenBank accession number NP694708). Peptides from the nine fragments covered 21% of the mouse EHD2 peptide sequence. Together, these data strongly suggest that the 65 kDa protein is EHD2 expressed in rat adipocytes. Similarly, MALDI-TOF MS of the tryptic fragments of the 230 kDa protein (band A in Figure 1B) indicated its potential identity with channel kinase 1 (GenBank accession number AAK19738), an α-kinase class protein kinase, whose function is associated with catalysis of autophosphorylation at the threonine residue (*42*). The 110 kDa protein (band B in Figure 1B) was identified as ADP-ribosyltransferase 1, an important regulatory component of the cellular response to DNA damage, expressed in rat (GenBank accession number NP037195) (*43*). Further identification and characterization of proteins A and B will be considered in separate reports.

To confirm whether EHD2 is authentically expressed in rat adipocytes, we performed RT-PCR in rat adipocytes using three different primer sets, EHD2-S1, -S2, and -S3, designed from highly conserved regions between human and mouse EHD2 sequences (see Experimental Procedures for the detailed sequences), using primer sets for β-actin as controls. The RT-PCR using the primers EHD2-S1, -S2, and -S3 produced the corresponding sizes of DNA segments from rat adipocyte mRNA (Figure 2A). Next, we sequenced these PCR products, designed primers from this sequence informa-

tion (see Experimental Procedures), and performed RACE PCR. The sequence information obtained from 5′ and 3′ RACE PCR was then used to design sense and antisense primers, respectively, which allowed PCR amplification of the complete open reading frame of rat adipose EHD2. The cDNA for rat adipose EHD2, which we have deposited in GenBank under accession number AF494093, contains an open reading frame from nucleotides 397 to 2004 which encodes 535 amino acids. The methionine at nucleotides 397−399 is almost certainly the site of initiation because there is an in-frame upstream stop codon at nucleotides 355−357, and the predicted size of the protein is in approximate agreement with its size, 65 kDa found by SDS gel electrophoresis. The sequence analysis of rat adipose EHD2 with the SMART program predicted the presence of an EH domain at the carboxyl terminus. The amino acid sequence of rat adipose EHD2 is 97.6% and 99.1% identical to that of human (AF214736) and mouse (AF155883) EHD2, respectively.

We next expressed and purified the His and GST fusion recombinant EHD2. His-EHD2 and GST-EHD2 migrated as 68 and 84 kDa bands in SDS−PAGE, respectively (not illustrated), consistent with the rat adipose EHD2 identified as the 65 kDa protein seen in the SDS gel of Figure 1. Polyclonal antibody was raised in rabbit using His fusion recombinant protein of rat adipocyte EHD2 as an antigen. The antibody was found to be highly specific for both His- and GST-EHD2 recombinant proteins (Figure 2B) without any cross-reactivity with the His or GST tag alone (data not shown). We purified EHD2-specific IgG from polyclonal serum using the affinity column coupled with GST-EHD2 fusion protein. In immunoblotting of rat adipocyte total lysates, this purified antibody reacted only with the 65 kDa band on the SDS gel (Figure 2C), indicating that EHD2 is indeed expressed in rat adipocytes.

Subcellular Distribution of EHD2 in Rat Adipocytes. Western blots using the purified EHD2 antibody described above revealed that EHD2 in adipocytes was mostly associated with membrane and particulate fractions, with only about 15% being found in the cytosol (Figure 3A). Approximately 15% of EHD2 in adipocytes was present in PM and 20%, 35%, and 17% were recovered in the NM, HDM, and LDM fractions, respectively. The exposure of adipocytes to insulin (100 nM, 37 °C, for 20 min) did not change the EHD2 abundance significantly in any of these fractions (Figure 3A).

We purified IRGTV from LDM using 1F8 and immunoblotted by EHD2 antibody to confirm the association of EHD2 with GLUT4-containing intracellular vesicles. The purified IRGTV displayed intense GLUT4 and IRAP immunoreactivities but no GLUT1 immunoreactivity (Figure 3B), demonstrating that the IRGTV used for analysis is highly specific for GLUT4. The EHD2 antibody stained a single, intense 65 kDa band in IRGTV upon immunoblotting (Figure 3B). Nonimmune IgG-coupled beads used as controls for the IRGTV purification did not show any positive signal in this blot (not shown). These results indicate that EHD2 is indeed associated with GLUT4-containing LDM vesicles in rat adipocytes.

To examine the possibility that the association of EHD2 with GLUT4 may be compartment-specific in rat adipocytes, we isolated the G, H, and L fractions by hypotonic lysis without homogenization (*9*) (also see Experimental Procedures), and GLUT4-containing vesicles in each of these fractions were purified by 1F8 immunoadsorption (as described in Experimental Procedures). Immunoblotting analyses of these GLUT4-containing vesicles using anti-EHD2 antibody revealed a single, immunostained protein with an apparent molecular mass of 65 kDa in each of the 1F8 adsorbates (Figure 4A), clearly demonstrating the association of EHD2 with the GLUT4 compartment in the G, H, and L fractions (designated as G4G, G4H, and G4L, respectively). When normalized against GLUT4 contents, the compartmental association of EHD2 with GLUT4 was two to three times greater in G4H than in $G4G_L$ or G4L (Figure 4B). Also shown in Figure 4A is that the majority of EHD2 was present in materials that were not adsorbed to 1F8 and were free of GLUT4, indicating that EHD2 binds mostly to the endosomal membranes that do not contain GLUT4.

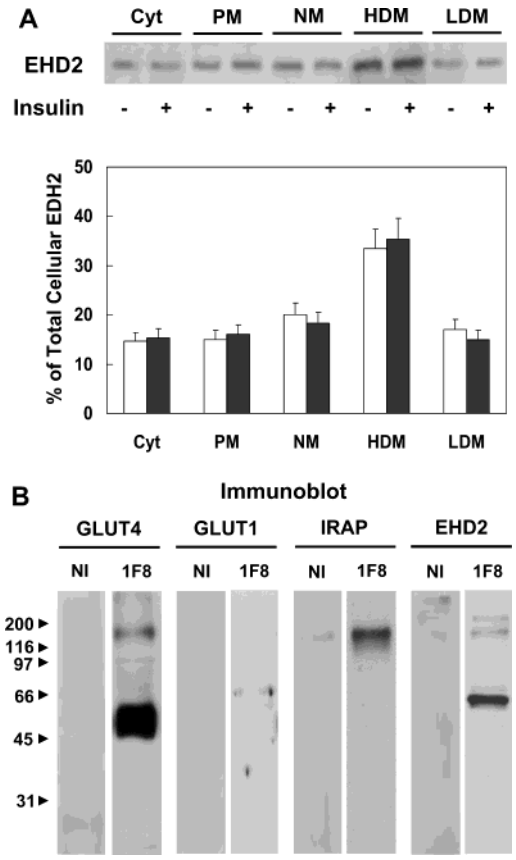

FIGURE 3: Subcellular distribution of EHD2 in rat adipocytes (panel A) and association of EHD2 with purified GLUT4 vesicles (IRGTV) from LDM (panel B). In panel A, the cytosol (Cyt), a plasma membrane-enriched fraction (PM), a nucleus/mitochondrial membrane-enriched fraction (NM), the high-density microsomes (HDM), and the low-density microsomes (LDM) were prepared from basal (−, open column) and insulin-stimulated (+, closed column) adipocytes as described in Experimental Procedures. One-twentieth amount of protein obtained from each fraction was subjected to immunoblot using purified antibodies raised against rat adipose His-EHD2 recombinant protein, and the percent distribution of EHD2 was measured from calculated total cellular EHD2. Results from five independent experiments were pooled, and the averages are shown with SD in vertical bars. In panel B, IRGTV was immunopurified from 200 μg of LDM of rat adipocytes using 30 μL of normal mouse IgG (NI) or 1F8-coupled (1F8) beads as described in Experimental Procedures. The proteins on IRGTV were resolved in SDS−PAGE in 8% gel and subjected to Western blotting with anti-GLUT4, GLUT1, IRAP, or EHD2 antibodies. Similar results were obtained in two other experiments.

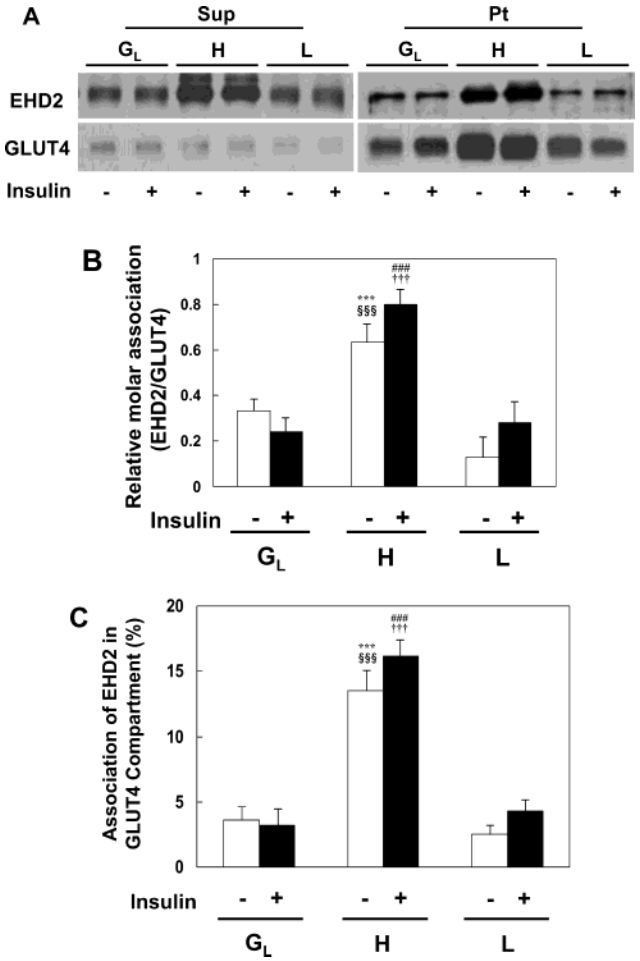

FIGURE 4: Relative abundance of EHD2 among GLUT4 vesicles purified from fractions G_L, H, and L in basal (−) and insulin-stimulated (+) rat adipocytes. In panel A, fractions G_L, H, and L were prepared and subjected to the 1F8 immunoadsorption (see Experimental Procedures), and the resulting supernatants (Sup) and immunoadsorbates (Pt) were immunoblotted using antibodies against rat adipose EHD2 (EHD2) or GLUT4 (GLUT4). Each lane contained fixed portions ($^1/_{50}$th for Sup and $^1/_{10}$th for Pt) of supernatants and adsorbates which originated from 200 μg of protein of the specified fraction. The relative molar association of EHD2 with GLUT4 (panel B) and the percentile participation of cellular EHD2 in GLUT4 compartments (panel C) were calculated from three independent experiments as illustrated in panel A above, and the averages were shown with SD in vertical bars in panels B and C. Key: (***) $p < 0.001$, compared to basal G_L; (###) $p < 0.001$, compared to insulin-stimulated G_L; (§§§) $p < 0.001$, compared to basal L; (†††) $p < 0.001$, compared to insulin-stimulated L.

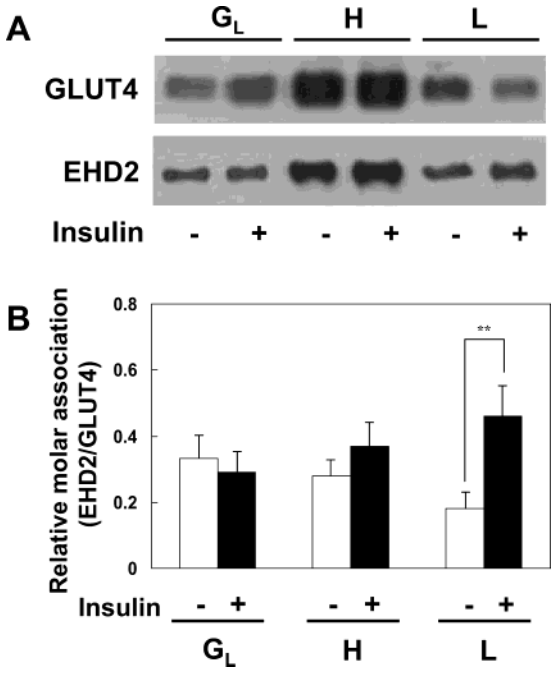

FIGURE 5: Co-immunoprecipitation of EHD2 and GLUT4 in intracellular GLUT4 compartments. In panel A, fractions G_L, H, and L were prepared (see Experimental Procedures) and subjected to immunoprecipitation with anti-EHD2 IgG. 80 μg of purified normal rabbit IgG or anti-EHD2 IgG (I) coupled on 80 μL of Trisacryl beads was incubated at 4 °C for 12 h with 600 μg of fractions G_L, H, and L containing 1% Triton X-100 from basal (−) or insulin-stimulated (+) adipocytes. The resulting immunoprecipitates were immunoblotted using antibodies against rat adipose GLUT4 (GLUT4) or EHD2 (EHD2). In panel B, the relative molar association of EHD2 with GLUT4 was calculated for each of fractions G_L, H, and L by dividing the EHD2 blot intensities by the GLUT4 blot intensities pooled from three experiments as illustrated in panel A, and the averages were shown with SD in vertical bars. Key: (**) $p < 0.01$, basal L versus insulin-stimulated L.

Quantitative analyses revealed that the GLUT4 compartment-associated EHD2 represents only a small fraction of the membrane-associated EHD2 in G, H, and L, typically accounting for 4%, 20%, and 5%, respectively (Figure 4C). A caveat is that as much as 40% of the GLUT4 pool in G was resistant to immunoadsorption. It is nevertheless worth noting that the compartmental association of EHD2 with GLUT4 was particularly high in H, the major insulin-sensitive, GLUT4-specific storage compartment in rat adipocytes.[2] Interestingly, the analyses also show that cellular insulin treatment resulted in a small but reproducible increase in the compartmental association of EHD2 with GLUT4 particularly in G4L and also in G4H, with a possible reduction, if any, in G4G (Figure 4B,C).

EHD2 Physically Interacts with GLUT4, and Insulin Modulates This Interaction in a Compartment-Specific Manner. EHD2 not only resides in GLUT4 compartments but also may physically interact with GLUT4 in these compartments. That this is the case was revealed in the following co-immunoprecipitation experiments (Figure 5). First G, H, and L ware prepared from basal (−) and insulin-stimulated (+) adipocytes, and then these individual subcellular fractions were immunoprecipitated using EHD2 antibody. When the immunoprecipitates were subjected to immunoblotting with GLUT4 and EHD2 antibodies, robust GLUT4 immunoreactivity was found in the EHD2 immunoprecipitates, along with EHD2 immunoreactivity in each fraction tested (Figure 5A). Most significantly, quantitative analyses of the blotting intensities revealed that the relative molar binding of EHD2 to GLUT4 was increased more than 2-fold in L, with an apparent slight increase in H and a possible decrease in G, respectively (Figure 5B). These findings and the findings of Figure 4B are consistent with the possibility that insulin stimulation affects the physical interaction of EHD2 with GLUT4 rather than the compartmental association of EHD2 with GLUT4 and in a compartment-specific manner.

EHD2 Also Interacts with μ_1, μ_2, and rCALM, the Adaptor Proteins Implicated in GLUT4 Recycling. We next examined

[2] C. Yu, J. Ryu, J. S. Samuel, W. Lee, and C. Y. Jung, unpublished data.

the possible interaction of EHD2 with other proteins involved in membrane protein recycling, namely, the clathrin adaptor middle chain subunits μ_1 and μ_2 and rCALM in vitro. These proteins have been shown to physically interact with GLUT4 and have been implicated in the regulation of the GLUT4 trafficking in rat adipocytes.[2] GST-μ_1, GST-μ_2, and GST-rCALM were incubated with the total lysate of rat adipocytes dissolved in 1% Triton X-100, and materials pulled down by the GST fusion proteins were subjected to immunoblotting with anti-EHD2 antibody (Figure 6A). GST-μ_1, GST-μ_2, and GST-rCALM pulled down endogenous EHD2 in adipocyte lysates, while GST alone did not, clearly demonstrating that EHD2 physically interacts with μ_1, μ_2, and rCALM in vitro.

The physical interactions of EHD2 with GLUT4 and rCALM were further confirmed in co-immunoprecipitation experiments using total adipocyte lysates (Figure 6B,C). GLUT4 antibody 1F8 coprecipitated both EHD2 and rCALM immunoreactivities along with GLUT4, while control nonimmune IgG did not (Figure 6B). Furthermore, our adipocyte EHD2 antibody similarly co-immunoprecipitated GLUT4 and rCALM immunoreactivity along with EHD2, while nonimmune IgG did not (Figure 6C). Immunoprecipitates with anti-EHD2 antibody did not show immunoreactivity against anti-IRAP antibody, indicating that EHD2 does not directly interact with IRAP (data not shown). These findings clearly indicate that EHD2 physically interacts with GLUT4 and rCALM. These interactions studied with adipocyte total lysates were not significantly affected by cellular treatment with insulin (Figure 6B,C).

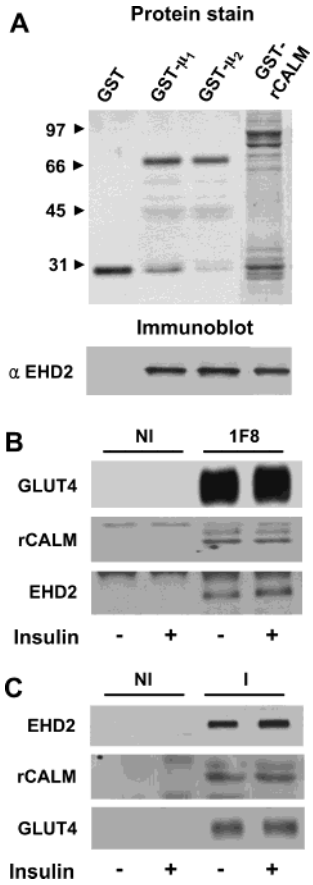

FIGURE 6: Interaction of μ_1, μ_2, and rCALM with endogenous EHD2 in vitro in GST pull-down experiments (panel A) and co-immunoprecipitation of EHD2 and GLUT4 with each other in rat adipocytes (panels B and C). In panel A, 5 μg of GST-μ_1, GST-μ_2, and GST-rCALM immobilized on glutathione−agarose beads was incubated with 1 mg (protein) of adipocyte total lysates in 1 mL of 150 mM PBS at 4 °C for 3 h with end-over-end rotation. The beads were then collected by centrifugation and washed three times with 1 mL of PBS. Proteins on the beads were eluted with 50 μL of 10 mM reduced glutathione in 50 mM Tris-HCl (pH 8.0). Proteins in the eluates were then separated by 8% SDS−PAGE and stained with Coomassie Blue for protein (upper panel) or immunoblotted with anti-EHD2 antibody (lower panel). Similar results were obtained in two other experiments. In panel B, adipocyte total lysates in dissolving buffer containing 1% Triton X-100 were prepared as described in Experimental Procedures. 30 μg of normal IgG (NI) or 1F8-coupled (1F8) beads (60 μL of 50% slurry) was incubated with 200 μg of LDM from basal (−) or insulin-stimulated (+) adipocytes in 500 μL of 150 mM PBS containing 1% Triton X-100 at 4 °C, overnight. Washed beads were mixed with 1 mg of adipocyte total cell lysates in 1 mL of 150 mM PBS at 4 °C for 3 h with end-over-end rotation. The beads were washed three times with 1 mL of PBS and subjected to GLUT4, rCALM, and EHD2 immunoblots. In panel C, 40 μg of purified normal rabbit IgG or anti-EHD2 IgG (I) coupled on 40 μL of Trisacryl beads (Reacti-Gel GF2000) was incubated at 4 °C for 12 h with 1 mg of total lysates containing 1% Triton X-100 from basal (−) or insulin-stimulated (+) adipocytes. The beads were washed three times with 1 mL of PBS containing 1% Triton X-100 and subjected to GLUT4 immunoblots. Similar results were obtained in two other experiments.

EHD2 Antibody and a Dominant Negative Mutant of EHD2 Introduced in Adipocytes Reduce Insulin-Induced GLUT4 Recruitment. To investigate the possible functional significance of the physical interaction and compartmental association of EHD2 with GLUT4 in insulin-induced GLUT4 recruitment, we introduced the affinity-purified anti-EHD2 antibody and GST fusion peptides containing the wild-type EHD2 or Eps15 homology domain (Glu^{428}−Glu^{535}) (GST-ΔEHD2) into rat adipocytes and studied their effects on the steady-state distribution of endogenous GLUT4 between the PM and the LDM (Figure 7). Basal and insulin-stimulated adipocytes were permeabilized using SLO in the absence and in the presence of normal rabbit IgG or purified anti-EHD2 antibody (0.5 mg/mL each) and GST, GST-EHD2, or GST-ΔEHD2 (50 μM each) (see Experimental Procedures for details), and then PM and LDM fractions were isolated and subjected to immunoblot with anti-GLUT4 antibody. Either in nonimmune IgG-incorporated adipocytes (Figure 7A) or in GST-incorporated adipocytes (Figure 7B), insulin increased the PM GLUT4 content 4.5−5-fold, with a concomitant reduction (by 25−30%) in the LDM GLUT4 pool size. These are essentially identical to the GLUT4 subcellular distributions observed in intact (nonpermeabilized) adipocytes and in SLO-treated adipocytes in the absence of nonimmune IgG or antibody (data not shown) as well. In anti-EHD2 antibody-incorporated adipocytes, however, there was a drastic (75%) reduction in the insulin-induced increase in PM GLUT4 content in host cells (Figure 7A), indicating that anti-EHD2 antibody inhibits insulin-induced GLUT4 recruitment to the plasma membrane. Introduction of wild-type GST-EHD2 protein (50 μM) to adipocytes did not change the basal GLUT4 level in PM, and insulin-induced GLUT4 translocation to PM was not increased significantly (data not shown). However, a less prominent but significant (35%) reduction in insulin-induced recruitment of GLUT4 to PM was observed in GST-ΔEHD2-incorporated adipocytes (Figure 7B). While the EHD2 antibody may have cross-linked GLUT4 vesicles, causing apparent inhibition of GLUT4 trafficking in these experi-

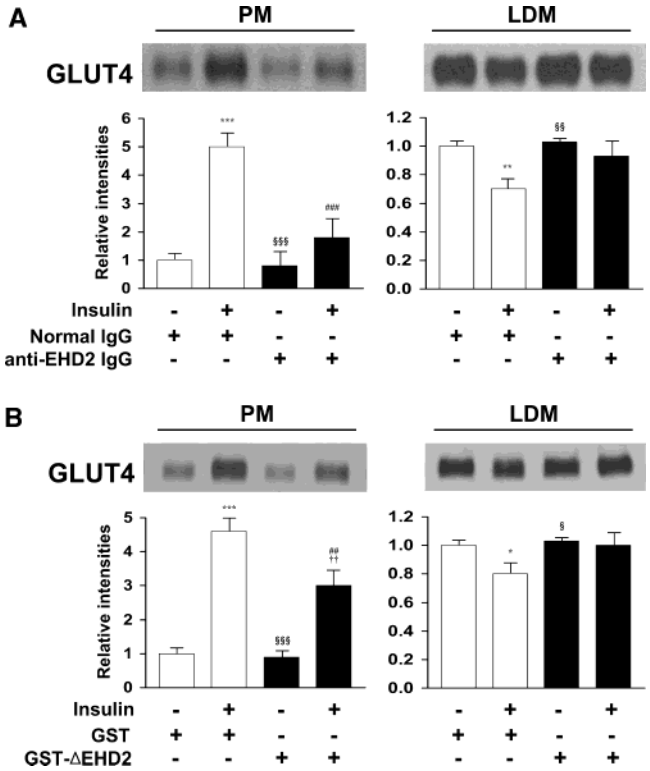

FIGURE 7: Effects of anti-EHD2 antibody or the partial segment of EHD2 (GST-ΔEHD2; Glu^{428}−Glu^{535}) on the basal and insulin-stimulated GLUT4 subcellular distribution in SLO-permeabilized rat adipocytes. Adipocytes were permeabilized with SLO (200 units/mL) and treated with anti-EHD2 IgG (0.5 mg/mL) (panel A) or GST-ΔEHD2 (50 μM) (panel B) as described in Experimental Procedures. When insulin was used, adipocytes were treated with insulin (100 nM) for the last 20 min of incubation. PM and LDM fractions were isolated from adipocytes after homogenization and subjected to GLUT4 immunoblot (upper panel). Each lane contained a fix portion of subcellular fractions ($^1/_{10}$th rat equivalence). Immunoblot intensities were quantitated by densitometry (see Experimental Procedures) and expressed in arbitrary units where the intensity of basal PM was 1. Results from four independent experiments were pooled, and the averages were shown with SD in vertical bars (lower panel). Key: (***) $p < 0.001$, (**) $p < 0.01$, (*) $p < 0.05$, compared to control basal; (###) $p < 0.001$, (##) $p < 0.01$, compared to control insulin; (§§§) $p < 0.001$, (§§) $p < 0.01$, (§) $p < 0.05$, compared to compared to control insulin; (††) $p < 0.01$, compared to GST-ΔEHD2 basal.

ments, the use of GST-ΔEHD2 should be free of this problem. Neither anti-EHD2 antibody nor GST-ΔEHD2 produced significant effects in the basal GLUT4 levels in PM and LDM in these experiments (Figure 7A,B), indicating that the effects are specific for insulin-stimulated GLUT4 recycling processes.

DISCUSSION

GLUT4 recycling and insulin-induced GLUT4 recruitment involve a series of complex membrane processes including GLUT4 sorting for the carrier-vesicle generation at a donor membrane and the carrier-vesicle movement and its subsequent fusion to the acceptor membrane (*1*, *44*). Each of these processes appears to be mediated by proteins (GLUT4 traffic regulatory proteins), some of which are modulated by the insulin signal. Some of these GLUT4 regulatory proteins are expected to interact with GLUT4 directly or indirectly and in a compartment-specific manner. Here we have identified a 65 kDa protein in GLUT4 vesicles immunopurified from the microsomal fraction of rat adipocytes (Figure 1) as EHD2. This identity was first indicated by MALDI-TOF MS tryptic fragmentation spectrum profile analysis and subsequently confirmed by RT-PCR (Figure 2A), gene cloning (GenBank accession number AF494093), and immunological cross-reactivity (Figure 2C).

EHD2 is a member of a highly conserved adaptor protein family known as the Eps15 homology domain- (EH domain-) containing protein (*45*). The EH domain (*46*, *47*) is an important protein−protein interaction motif thought to be involved in intracellular sorting (*48*). The EH domain-containing proteins are associated with the plasma membrane adaptor complex, AP-2, suggesting their role in clathrin-mediated endocytosis (*48*−*50*). Dominant negative mutation or RNAi-mediated interference of RME-1, the EHD1 expressed in *Caenorhabditis elegans*, caused dispersal of the endosomal recycling compartments and slowed internalized receptor recycling to the plasma membrane, suggesting its role in the molecular machinery responsible for the return of recycling protein from the endosomal compartment to the plasma membrane (*51*, *52*). More recently, several investigators (*53*−*55*) have shown that EHD1 participates in recycling of internalized plasma membrane proteins by inducing tubule formation with Arf6 in the clathrin-independent endocytosis. There is a growing number of EH domain-containing proteins, including Eps15 (*46*, *47*), intersectins (*56*), Reps (*57*), POB1 (*53*), *Drosophila* PAST-1 (*48*), Dap 160 protein (*54*), and *C. elegans* RME-1 (*51*, *52*), all thought to be associated with intracellular routing and endocytosis.

Human and mouse EHD1 has been cloned and shown to be ubiquitously expressed in human cells (*58*). Subsequently, EHD2, EHD3, and EHD4 have been cloned by screening of a human fetal brain cDNA library (*45*). All members of this family have three highly conserved domains: an N-terminal P-loop domain containing nucleotide-binding motifs, a central region with high probability of forming coiled coils, and a C-terminal EH domain (*45*, *49*, *58*). In the present study, we have cloned and purified 535 amino acid long EHD2 in rat adipocytes (AF494093), which is 97.6% and 99.1% identical to human (AF214736) and mouse (AF155883) EHD2, respectively. The protein alignment and motif search analysis revealed that rat adipocyte EHD2 contains an EH domain in the carboxyl terminus that includes an EF hand, a Ca^{2+}-binding motif, a central coiled-coil region, and a nucleotide-binding consensus site at the N-terminal domain.

EHD2 in rat adipocytes is predominantly (more than 85%) membrane-associated (Figure 3), including the plasma membranes and all of the intracellular membrane fractions tested (Figure 3A). This is consistent with the finding that EHD1 in several mammalian cell lines is localized in various cytoplasmic vesicular structures including organelle membrane, tubular structures, endocytic vesicles, and Golgi apparatus (*53*, *58*). No morphological data are currently available on the subcellular localization of EHD2 in mammalian cells.

EHD2 is a major resident protein in the endosomal GLUT4 vesicles in adipocytes (Figure 1). This compartmental association of EHD2 with GLUT4 was also readily demonstrable in EHD2 immunoblots of GLUT4 vesicles purified from the LDM fraction (Figure 3B). This association was uniformly observed with all of the GLUT4 pools (compartments) in three individual subcellular fractions tested,

namely, G, H, and L (Figure 4A). The compartmental association of EHD2 with GLUT4, however, shows certain interesting differences among different GLUT4 pools: First, EHD2 is particularly enriched in the GLUT4 compartment in fraction H (G4H) than in G4G or G4L (Figure 4B); the molar association of EHD2 with GLUT4 was 2−3.5-fold greater in G4H than in G4G and G4L (Figure 4B). Second, the molar association of EHD2 with GLUT4 was 2-fold greater in G4L in insulin-stimulated cells.

Finally, most of the membrane association of EHD2 occurs outside the GLUT4 compartments (Figure 4B). The EHD2 associated with GLUT4 compartment amounts to not more than 5% in G and L fractions, although it was as high as 15% in H (Figure 4C). This finding is consistent with the observation that EHD1 and EHD3 are largely associated with transferrin-enriched cytoplasmic tubular structures regarded as the recycling endosomal compartments of the constitutive recycling pathway (*55*). It is thus likely that EHD2 in adipocytes is involved not only in GLUT4 recycling but also in other membrane protein recycling of constitutive recycling pathway.

It is clear in co-immunoprecipitation experiments that EHD2 physically interacts with GLUT4 in these compartments (Figure 5). We do not know whether all or part of the EHD2 in the GLUT4 compartment directly interacts with GLUT4. This physical interaction occurred in each of the GLUT4 pools tested as revealed (Figure 5A). More importantly, this direct interaction of EHD2 with GLUT4 was affected by cellular insulin treatment, showing a 2.5-fold increase in the GLUT4 pool in L (G4L), with a slight (5−10%) increase in the GLUT4 pool in H (G4H) (Figure 5B). This insulin-induced, apparently G4L-selective, enhancement in the molecular interaction of EHD2 with GLUT4 is consistent with the similar insulin effects observed in EHD2-GLUT4 compartmental association (Figure 4B).

We have previously shown that G4H and G4L are two major GLUT4 storage compartments from which insulin recruits GLUT4 to the plasma membrane (*9*, *31*, *32*). G4H is free from GLUT1 (*31*) and transferrin receptor,[2] indicating that it is a GLUT4-specific compartment, clearly different from the recycling endosomal compartment of the constitutive recycling pathway. G4L is also free of GLUT1 and transferrin receptor[2] and most likely represents the GLUT4 exocytic vesicles en route to the plasma membrane.[2] The large and reproducible increase in the molecular interaction (Figure 5B) as well as the compartmental association (Figure 4B) of EHD2 with GLUT4 in G4L (and also, to a less extent, in G4H) observed upon cellular insulin treatment strongly suggests the physiological relevance of this interaction. Interestingly, anti-EHD2 antibody in permeabilized rat adipocytes drastically (more than 75%) reduced insulin-induced GLUT4 recruitment without affecting basal GLUT4 distribution (Figure 7A). Similarly, the GST fusion protein of ΔEHD2, a dominant negative mutant of EHD2, also inhibited the insulin-induced GLUT4 recruitment in permeabilized rat adipocytes by 35% without affecting basal GLUT4 distribution (Figure 7B). This strongly suggests that EHD2 is indeed involved in insulin-induced GLUT4 recruitment in rat adipocytes. How and in which of the compartments or steps in the GLUT4 trafficking itinerary EHD2 participates in insulin-induced GLUT4 recruitment remain to be investigated. Quantitative assessments of the changes in the steady-state GLUT4 pool sizes in G, T, and L fractions (*31*, *59*) brought by EDH2 antibody or ΔEHD2 injection may provide a clue to answer these questions, and these experiments are currently underway in our laboratory.

The molecular events underlying the EHD2 participation in GLUT4 trafficking postulated above are yet to be identified and can only be speculated at this time. The observed reduction in the insulin-induced GLUT4 recruitment caused by anti-EHD2 antibody or ΔEHD2 (Figure 7) is consistent with the possibility that EHD2 interacts with GLUT4 as an essential step in targeting GLUT4 to the clathrin-coated, carrier-vesicle generation during the GLUT4 transit from endosomes to the plasma membrane and that the antibody or ΔEHD2 interferes with this EHD2-GLUT4 interaction. Our findings that EHD2 interacts not only with GLUT4 but also with the AP subunit μ_1 or μ_2 and rCALM (Figure 6) further suggest the involvement of these adaptor proteins in this process. AP-1 interacts with GLUT4 and GLUT4 vesicles isolated from adipocytes where the subunit μ_1 or μ_2 recognizes the GLUT4 C-terminal cytoplasmic domain[3] and may be responsible for selective GLUT4 targeting to the clathrin-coated carrier-vesicle budding during the endosomal GLUT4 trafficking (*60*, *61*). rCALM (*62*) is a nonneuronal homologue of AP180, a clathrin-assembly protein originally isolated from synaptic vesicles (*63*−*65*) that binds to clathrin and promotes clathrin coat assembly in vitro (*66*). CALM is also implicated in the clathrin-mediated endocytosis (*67*). Similar to EHD2 in rat adipocytes, CALM in HeLa cells was more than 85% membrane-associated and colocalized with AP-2 but not with AP-1 (*67*). Furthermore, overexpression of CALM or its fragments inhibited the endocytosis of transferrin and epidermal growth factor receptors (*67*). More recently, CALM was shown to bind to the membrane lipid PtdIns(4,5)P_2 at its N-terminal ENTH (epsin N-terminal homology) domain (*68*) and, together with its binding to clathrin, may initiate clathrin-coated pit formation for endocytosis (*69*). Clearly, much work is needed to determine if or how the interaction of EHD2 with AP-1/AP-2 and the adaptor-associated proteins rCALM described here is related to the compartmental association of EHD2 with GLUT4 and its possible role in GLUT4 trafficking in adipocytes.

[3] J. Ryu, J. S. Samuel, W. Lee, and C. Y. Jung, unpublished data.

REFERENCES

1. Pessin, J. E., and Saltiel, A. R. (2000) Signaling pathways in insulin action: molecular targets of insulin resistance, *J. Clin. Invest. 106*, 165−169.
2. James, D. E., Strube, M., and Mueckler, M. (1989) Molecular cloning and characterization of an insulin-regulatable glucose transporter, *Nature 338*, 83−87.
3. Cushman, S. W., and Wardzala, L. J. (1980) Potential mechanism of insulin action on glucose transport in the isolated rat adipose cell. Apparent translocation of intracellular transport systems to the plasma membrane, *J. Biol. Chem. 255*, 4758−4762.
4. Jhun, B. H., Rampal, A. L., Liu, H., Lachaal, M., and Jung, C. Y. (1992) Effects of insulin on steady-state kinetics of GLUT4 subcellular distribution in rat adipocytes. Evidence of constitutive GLUT4 recycling, *J. Biol. Chem. 267*, 17710−17715.
5. Czech, M. P., and Corvera, S. (1999) Signaling mechanisms that regulate glucose transport, *J. Biol. Chem. 274*, 1865−1868.
6. Pessin, J. E., Thurmond, D. C., Elmendorf, J. S., Coker, K. J., and Okada, S. (1999) Molecular basis of insulin-stimulated

GLUT4 vesicle trafficking. Location! Location! Location!, *J. Biol. Chem. 274*, 2593−2596.
7. Slot, J. W., Geuze, H. J., Gigengack, S., Lienhard, G. E., and James, D. E. (1991) Immuno-localization of the insulin regulatable glucose transporter in brown adipose tissue of the rat, *J. Cell Biol. 113*, 123−135.
8. Smith, R. M., Charron, M. J., Shah, N., Lodish, H. F., and Jarett, L. (1991) Immunoelectron microscopic demonstration of insulin-stimulated translocation of glucose transporters to the plasma membrane of isolated rat adipocytes and masking of the carboxyl-terminal epitope of intracellular GLUT4, *Proc. Natl. Acad. Sci. U.S.A. 88*, 6893−6897.
9. Lee, W., Ryu, J., Souto, R. P., Pilch, P. F., and Jung, C. Y. (1999) Separation and partial characterization of three distinct intracellular GLUT4 compartments in rat adipocytes. Subcellular fractionation without homogenization, *J. Biol. Chem. 274*, 37755−37762.
10. Lee, W., Ryu, J., Spangler, R. A., and Jung, C. Y. (2000) Modulation of GLUT4 and GLUT1 recycling by insulin in rat adipocytes: kinetic analysis based on the involvement of multiple intracellular compartments, *Biochemistry 39*, 9358−9366.
11. Martin, S., Tellam, J., Livingstone, C., Slot, J. W., Gould, G. W., and James, D. E. (1996) The glucose transporter (GLUT-4) and vesicle-associated membrane protein-2 (VAMP-2) are segregated from recycling endosomes in insulin-sensitive cells, *J. Cell Biol. 134*, 625−635.
12. Olson, A. L., Knight, J. B., and Pessin, J. E. (1997) Syntaxin 4, VAMP2, and/or VAMP3/cellubrevin are functional target membrane and vesicle SNAP receptors for insulin-stimulated GLUT4 translocation in adipocytes, *Mol. Cell. Biol. 17*, 2425−2435.
13. Cheatham, B., Volchuk, A., Kahn, C. R., Wang, L., Rhodes, C. J., and Klip, A. (1996) Insulin-stimulated translocation of GLUT4 glucose transporters requires SNARE-complex proteins, *Proc. Natl. Acad. Sci. U.S.A. 93*, 15169−15173.
14. Laurie, S. M., Cain, C. C., Lienhard, G. E., and Castle, J. D. (1993) The glucose transporter GluT4 and secretory carrier membrane proteins (SCAMPs) colocalize in rat adipocytes and partially segregate during insulin stimulation, *J. Biol. Chem. 268*, 19110−19117.
15. Kandror, K. V., Coderre, L., Pushkin, A. V., and Pilch, P. F. (1995) Comparison of glucose-transporter-containing vesicles from rat fat and muscle tissues: evidence for a unique endosomal compartment, *Biochem. J. 307* (Part 2), 383−390.
16. Kupriyanova, T. A., and Kandror, K. V. (2000) Cellugyrin is a marker for a distinct population of intracellular Glut4-containing vesicles, *J. Biol. Chem. 275*, 36263−36268.
17. Kupriyanova, T. A., Kandror, V., and Kandror, K. V. (2002) Isolation and characterization of the two major intracellular Glut4 storage compartments, *J. Biol. Chem. 277*, 9133−9138.
18. Kandror, K. V., and Pilch, P. F. (1996) The insulin-like growth factor II/mannose 6-phosphate receptor utilizes the same membrane compartments as GLUT4 for insulin-dependent trafficking to and from the rat adipocyte cell surface, *J. Biol. Chem. 271*, 21703−21708.
19. Kandror, K. V., and Pilch, P. F. (1998) Multiple endosomal recycling pathways in rat adipose cells, *Biochem. J. 331* (Part 3), 829−835.
20. Lin, B. Z., Pilch, P. F., and Kandror, K. V. (1997) Sortilin is a major protein component of Glut4-containing vesicles, *J. Biol. Chem. 272*, 24145−24147.
21. Garza, L. A., and Birnbaum, M. J. (2000) Insulin-responsive aminopeptidase trafficking in 3T3-L1 adipocytes, *J. Biol. Chem. 275*, 2560−2567.
22. Sleeman, M. W., Donegan, N. P., Heller-Harrison, R., Lane, W. S., and Czech, M. P. (1998) Association of acyl-CoA synthetase-1 with GLUT4-containing vesicles, *J. Biol. Chem. 273*, 3132−3135.
23. Calera, M. R., Martinez, C., Liu, H., Jack, A. K., Birnbaum, M. J., and Pilch, P. F. (1998) Insulin increases the association of Akt-2 with Glut4-containing vesicles, *J. Biol. Chem. 273*, 7201−7204.
24. Kupriyanova, T. A., and Kandror, K. V. (1999) Akt-2 binds to Glut4-containing vesicles and phosphorylates their component proteins in response to insulin, *J. Biol. Chem. 274*, 1458−1464.
25. Cormont, M., Tanti, J. F., Zahraoui, A., Van Obberghen, E., Tavitian, A., and Le Marchand-Brustel, Y. (1993) Insulin and okadaic acid induce Rab4 redistribution in adipocytes, *J. Biol. Chem. 268*, 19491−19497.
26. Kessler, A., Tomas, E., Immler, D., Meyer, H. E., Zorzano, A., and Eckel, J. (2000) Rab11 is associated with GLUT4-containing vesicles and redistributes in response to insulin, *Diabetologia 43*, 1518−1527.
27. Heller-Harrison, R. A., Morin, M., Guilherme, A., and Czech, M. P. (1996) Insulin-mediated targeting of phosphatidylinositol 3-kinase to GLUT4-containing vesicles, *J. Biol. Chem. 271*, 10200−10204.
28. Del Vecchio, R. L., and Pilch, P. F. (1991) Phosphatidylinositol 4-kinase is a component of glucose transporter (GLUT 4)-containing vesicles, *J. Biol. Chem. 266*, 13278−13283.
29. Shisheva, A., Buxton, J., and Czech, M. P. (1994) Differential intracellular localizations of GDP dissociation inhibitor isoforms. Insulin-dependent redistribution of GDP dissociation inhibitor-2 in 3T3-L1 adipocytes, *J. Biol. Chem. 269*, 23865−23868.
30. Chi, N. W., and Lodish, H. F. (2000) Tankyrase is a golgi-associated mitogen-activated protein kinase substrate that interacts with IRAP in GLUT4 vesicles, *J. Biol. Chem. 275*, 38437−38444.
31. Lee, W., Ryu, J., Hah, J., Tsujita, T., and Jung, C. Y. (2000) Association of carboxyl esterase with facilitative glucose transporter isoform 4 (GLUT4) intracellular compartments in rat adipocytes and its possible role in insulin-induced GLUT4 recruitment, *J. Biol. Chem. 275*, 10041−10046.
32. Guilherme, A., Emoto, M., Buxton, J. M., Bose, S., Sabini, R., Theurkauf, W. E., Leszyk, J., and Czech, M. P. (2000) Perinuclear localization and insulin responsiveness of GLUT4 requires cytoskeletal integrity in 3T3-L1 adipocytes, *J. Biol. Chem. 275*, 38151−38159.
33. Bose, A., Guilherme, A., Robida, S. I., Nicoloro, S. M., Zhou, Q. L., Jiang, Z. Y., Pomerleau, D. P., and Czech, M. P. (2002) Glucose transporter recycling in response to insulin is facilitated by myosin Myo1c, *Nature 420*, 821−824.
34. James, D. E., Brown, R., Navarro, J., and Pilch, P. F. (1988) Insulin-regulatable tissues express a unique insulin-sensitive glucose transport protein, *Nature 333*, 183−185.
35. Liu, H., Xiong, S., Shi, Y., Samuel, S. J., Lachaal, M., and Jung, C. Y. (1995) ATP-sensitive binding of a 70-kDa cytosolic protein to the glucose transporter in rat adipocytes, *J. Biol. Chem. 270*, 7869−7875.
36. Martz, A., Mookerjee, B. K., and Jung, C. Y. (1986) Insulin and phorbol esters affect the maximum velocity rather than the half-saturation constant of 3-O-methylglucose transport in rat adipocytes, *J. Biol. Chem. 261*, 13606−13609.
37. Laemmli, U. K. (1970) Cleavage of structural proteins during the assembly of the head of bacteriophage T4, *Nature 227*, 680−685.
38. Schoenle, E. J., Adams, L. D., and Sammons, D. W. (1984) Insulin-induced rapid decrease of a major protein in fat cell plasma membranes, *J. Biol. Chem. 259*, 12112−12116.
39. Yates, J. R., III (1998) Mass spectrometry and the age of the proteome, *J. Mass Spectrom. 33*, 1−19.
40. Chomczynski, P., and Sacchi, N. (1987) Single-step method of RNA isolation by acid guanidinium thiocyanate-phenol-chloroform extraction, *Anal. Biochem. 162*, 156−159.
41. Martin, L. B., Shewan, A., Millar, C. A., Gould, G. W., and James, D. E. (1998) Vesicle-associated membrane protein 2 plays a specific role in the insulin-dependent trafficking of the facilitative glucose transporter GLUT4 in 3T3-L1 adipocytes, *J. Biol. Chem. 273*, 1444−1452.
42. Ryazanov, A. G., Pavur, K. S., and Dorovkov, M. V. (1999) Alpha-kinases: a new class of protein kinases with a novel catalytic domain, *Curr. Biol. 9*, R43−R45.
43. Beneke, S., Meyer, R., and Burkle, A. (1997) Isolation of cDNA encoding full-length rat (Rattus norvegicus) poly (ADP-ribose) polymerase, *Biochem. Mol. Biol. Int. 43*, 755−761.
44. Bryant, N. J., Govers, R., and James, D. E. (2002) Regulated transport of the glucose transporter GLUT4, *Nat. Rev. Mol. Cell Biol. 3*, 267−277.
45. Pohl, U., Smith, J. S., Tachibana, I., Ueki, K., Lee, H. K., Ramaswamy, S., Wu, Q., Mohrenweiser, H. W., Jenkins, R. B., and Louis, D. N. (2000) EHD2, EHD3, and EHD4 encode novel members of a highly conserved family of EH domain-containing proteins, *Genomics 63*, 255−262.
46. Fazioli, F., Minichiello, L., Matoskova, B., Wong, W. T., and Di Fiore, P. P. (1993) eps15, a novel tyrosine kinase substrate, exhibits transforming activity, *Mol. Cell. Biol. 13*, 5814−5828.
47. Wong, W. T., Schumacher, C., Salcini, A. E., Romano, A., Castagnino, P., Pelicci, P. G., and Di Fiore, P. (1995) A protein-binding domain, EH, identified in the receptor tyrosine kinase substrate Eps15 and conserved in evolution, *Proc. Natl. Acad. Sci. U.S.A. 92*, 9530−9534.

48. Di Fiore, P. P., Pelicci, P. G., and Sorkin, A. (1997) EH: a novel protein−protein interaction domain potentially involved in intracellular sorting, *Trends Biochem. Sci. 22*, 411−413.
49. Santolini, E., Salcini, A. E., Kay, B. K., Yamabhai, M., and Di Fiore, P. P. (1999) The EH network, *Exp. Cell Res. 253*, 186−209.
50. Mayer, B. J. (1999) Endocytosis: EH domains lend a hand, *Curr. Biol. 9*, R70−R73.
51. Lin, S. X., Grant, B., Hirsh, D., and Maxfield, F. R. (2001) Rme-1 regulates the distribution and function of the endocytic recycling compartment in mammalian cells, *Nat. Cell Biol. 3*, 567−572.
52. Grant, B., Zhang, Y., Paupard, M. C., Lin, S. X., Hall, D. H., and Hirsh, D. (2001) Evidence that RME-1, a conserved C. elegans EH-domain protein, functions in endocytic recycling, *Nat. Cell Biol. 3*, 573−579.
53. Ikeda, M., Ishida, O., Hinoi, T., Kishida, S., and Kikuchi, A. (1998) Identification and characterization of a novel protein interacting with Ral-binding protein 1, a putative effector protein of Ral, *J. Biol. Chem. 273*, 814−821.
54. Roos, J., and Kelly, R. B. (1998) Dap160, a neural-specific Eps15 homology and multiple SH3 domain-containing protein that interacts with Drosophila dynamin, *J. Biol. Chem. 273*, 19108−19119.
55. Caplan, S., Naslavsky, N., Hartnell, L. M., Lodge, R., Polishchuk, R. S., Donaldson, J. G., and Bonifacino, J. S. (2002) A tubular EHD1-containing compartment involved in the recycling of major histocompatibility complex class I molecules to the plasma membrane, *EMBO J. 21*, 2557−2567.
56. Okamoto, M., Schoch, S., and Sudhof, T. C. (1999) EHSH1/intersectin, a protein that contains EH and SH3 domains and binds to dynamin and SNAP-25. A protein connection between exocytosis and endocytosis?, *J. Biol. Chem. 274*, 18446−18454.
57. Yamaguchi, A., Urano, T., Goi, T., and Feig, L. A. (1997) An Eps homology (EH) domain protein that binds to the Ral-GTPase target, RalBP1, *J. Biol. Chem. 272*, 31230−31234.
58. Mintz, L., Galperin, E., Pasmanik-Chor, M., Tulzinsky, S., Bromberg, Y., Kozak, C. A., Joyner, A., Fein, A., and Horowitz, M. (1999) EHD1−an EH-domain-containing protein with a specific expression pattern, *Genomics 59*, 66−76.
59. Hah, J. S., Ryu, J. W., Lee, W., Kim, B. S., Lachaal, M., Spangler, R. A., and Jung, C. Y. (2002) Transient changes in four GLUT4 compartments in rat adipocytes during the transition, insulin-stimulated to basal: implications for the GLUT4 trafficking pathway, *Biochemistry 41*, 14364−14371.
60. Al-Hasani, H., Kunamneni, R. K., Dawson, K., Hinck, C. S., Muller-Wieland, D., and Cushman, S. W. (2002) Roles of the N- and C-termini of GLUT4 in endocytosis, *J. Cell Sci. 115*, 131−140.
61. Gillingham, A. K., Koumanov, F., Pryor, P. R., Reaves, B. J., and Holman, G. D. (1999) Association of AP1 adaptor complexes with GLUT4 vesicles, *J. Cell Sci. 112* (Part 24), 4793−4800.
62. Kim, J. A., Kim, S. R., Jung, Y. K., Woo, S. Y., Seoh, J. Y., Hong, Y. S., and Kim, H. L. (2000) Properties of GST-CALM expressed in E. coli, *Exp. Mol. Med. 32*, 93−99.
63. Dreyling, M. H., Martinez-Climent, J. A., Zheng, M., Mao, J., Rowley, J. D., and Bohlander, S. K. (1996) The t(10;11)(p13;q14) in the U937 cell line results in the fusion of the AF10 gene and CALM, encoding a new member of the AP-3 clathrin assembly protein family, *Proc. Natl. Acad. Sci. U.S.A. 93*, 4804−4809.
64. Keen, J. H., and Black, M. M. (1986) The phosphorylation of coated membrane proteins in intact neurons, *J. Cell Biol. 102*, 1325−1333.
65. Takei, K., Mundigl, O., Daniell, L., and De Camilli, P. (1996) The synaptic vesicle cycle: a single vesicle budding step involving clathrin and dynamin, *J. Cell Biol. 133*, 1237−1250.
66. Lindner, R., and Ungewickell, E. (1992) Clathrin-associated proteins of bovine brain coated vesicles. An analysis of their number and assembly promoting activity, *J. Biol. Chem. 267*, 16567−16573.
67. Tebar, F., Bohlander, S. K., and Sorkin, A. (1999) Clathrin assembly lymphoid myeloid leukemia (CALM) protein: localization in endocytic-coated pits, interactions with clathrin, and the impact of overexpression on clathrin-mediated traffic, *Mol. Biol. Cell 10*, 2687−2702.
68. Itoh, T., Koshiba, S., Kigawa, T., Kikuchi, A., Yokoyama, S., and Takenawa, T. (2001) Role of the ENTH domain in phosphatidylinositol-4,5-bisphosphate binding and endocytosis, *Science 291*, 1047−1051.
69. Ford, M. G., Pearse, B. M., Higgins, M. K., Vallis, Y., Owen, D. J., Gibson, A., Hopkins, C. R., Evans, P. R., and McMahon, H. T. (2001) Simultaneous binding of PtdIns(4,5)P2 and clathrin by AP180 in the nucleation of clathrin lattices on membranes, *Science 291*, 1051−1055.

BI049970F